Sensors and Materials, Vol. 38, No. 2 (2026) 603–608
MYU Tokyo

S & M 4328

Effect of Eu Doping on the Radiophotoluminescence Properties of $CaSiO_3$

Haruna Nogawa,[1*] Hidehito Nanto,[2] and Go Okada[1,2]

[1]Department of Chemistry and Environmental Science, Kanazawa Institute of Technology,
7-1 Ohgigaoka, Nonoichi, Ishikawa 921-8501, Japan
[2]Co-creative Research Center of Industrial Science and Technology, Kanazawa Institute of Technology,
3-1 Yatsukaho, Hakusan, Ishikawa 924-0838, Japan

(Received November 1, 2025; accepted December 16, 2025)

Keywords: radiophotoluminescence, RPL, Eu, $CaSiO_3$, X-ray

To explore new radiophotoluminescence (RPL) materials, Eu-doped $CaSiO_3$ was synthesized by a solid-state reaction method, and its RPL behavior was evaluated from the viewpoint of radiation detection applications. X-ray diffraction (XRD) analysis confirmed that all samples were single-phase $CaSiO_3$. After X-ray irradiation, a broad emission band attributed to the formation of Eu^{2+} centers was observed, indicating that the Eu-doped $CaSiO_3$ host material exhibits distinct RPL behavior. The RPL sensitivity to radiation was highest at an Eu concentration of 0.1 mol%, with a linear dose response range from 0.18 Gy to at least 10 Gy. The Eu^{2+} centers generated by irradiation were highly stable, showing only a 7% signal decrease after 20 min. Upon heat treatment, the photoluminescence (PL) spectra exhibited significant changes, accompanied by the emergence of a new broad emission band. Analysis revealed a decrease in the Eu^{2+} emission and a corresponding increase in the Eu^{3+} emission, suggesting a possible valence change from Eu^{2+} to Eu^{3+}. Furthermore, this broad emission becomes prominent at around 300 °C and above 400 °C and is also observed in undoped samples. The emission is considered to originate from defect centers formed within the host material during heat treatment.

1. Introduction

Radiophotoluminescence (RPL) is a phenomenon in which new luminescent centers are generated in a material through interactions with ionizing radiation.(1) The generated centers can be easily detected using conventional photoluminescence (PL) techniques, and the PL intensity is known to increase proportionally with the radiation dose delivered to the material.(2) Owing to this property, RPL has been widely utilized for precise radiation dosimetry. A notable advantage of successful RPL is that the generated luminescent centers are highly stable against external factors such as ambient light and temperature, as well as excitation light during readout. This stability allows repeated and nondestructive signal readout, which effectively reduces statistical

---

[*] Corresponding author: e-mail: c1227844@st.kanazawa-it.ac.jp
https://doi.org/10.18494/SAM6029

ISSN 0914-4935
https://myukk.org/

uncertainty. This is a notable advantage compared with other dosimetric approaches such as thermally stimulated luminescence (TSL) and optically stimulated luminescence (OSL), which require the release of trapped charges upon stimulation to read out the signal.(3,4) Despite its advantages, the number of known RPL materials suitable for dosimetric applications remains very limited. Representative examples include Ag-doped phosphate glass,(5–7) LiF,(8) and Al_2O_3:C,Mg.(9) Owing to this scarcity, the fundamental mechanisms underlying RPL and the material design principles remain insufficiently understood, hindering the exploration of new materials and the extension of RPL applications. Therefore, the discovery of new RPL materials and the elucidation of their fundamental properties are important.

In recent years, RPL phenomena have been reported in several inorganic compounds doped with rare-earth ions such as Sm, Eu, and Yb, as well as in some undoped compounds.(10–13) Silicate compounds are an interesting class of materials with outstanding optical, thermal, mechanical, and chemical properties. Among them, $CaSiO_3$ exhibits high chemical and thermal stability, and its polymorphic nature with multiple Ca^{2+} sites allows for the facile substitution of rare-earth ions. In addition, the rigid framework composed of SiO_4 tetrahedra can stably accommodate luminescent centers, making $CaSiO_3$ an excellent host material in terms of both structural and luminescent properties.(14,15) In this paper, we report a new RPL material, Eu-doped $CaSiO_3$, which exhibits the reduction of Eu^{3+} to Eu^{2+} under X-ray irradiation. The Eu-doped $CaSiO_3$ samples were synthesized by a conventional solid-state reaction method, and their phase purity, PL, and RPL characteristics were systematically investigated. Furthermore, the effects of heat treatment on the luminescence behavior were examined to clarify the underlying mechanisms of defect formation and valence-state changes.

2. Experimental Procedure

Eu-doped $CaSiO_3$ was synthesized by a solid-state reaction method. The starting raw materials, $CaCO_3$ (99.99%, Kojundo Chemical), SiO_2 (99.9%, Furuuchi Chemical), and Eu_2O_3 (99.9%, Kojundo Chemical), were weighed in accordance with the stoichiometric ratio as $Ca_{1-x}Eu_xSiO_3$ (x = 0.02, 0.05, 0.1, 0.2, 0.5 mol%). After weighing, the powders were wet-mixed with distilled water using an alumina mortar and pestle for 20 min. The obtained mixture was placed in an alumina crucible and calcined using an electric furnace (FT-105FM-ST, FULL-TECH). The calcination conditions were set at 1250 °C for 4 h in air. The sintering temperature was determined as 80% of its melting temperature (1540 °C). The obtained product was thoroughly ground into a fine powder for subsequent characterization.

The crystal structure of the synthesized samples was analyzed by powder X-ray diffraction (XRD). XRD patterns were recorded using a diffractometer (Ultima IV, Rigaku) equipped with a micro-focus X-ray tube (CuKα, λ = 1.54056 Å). The X-ray tube was operated at 30 kV and 20 mA. The obtained diffraction patterns were analyzed by comparison with reference patterns from the Powder Diffraction File (PDF) for phase identification.

Furthermore, RPL properties were evaluated using a TSL/OSL/RPL automatic integrated measurement system (TORAIMS).(16) This system enables automated operations such as PL spectrum measurement, X-ray irradiation, and thermal treatments, minimizing errors caused by human factors. The samples were excited by light at 340 ± 40 nm using a xenon lamp (LAX-C100, Asahi Spectra), and PL emissions were detected and recorded with a multichannel spectrometer (QEPro, Ocean Optics). X-ray irradiation was performed using a tungsten-anode X-ray tube (XRB80N100B, Spellman) operated at a fixed voltage of 40 kV, with the tube current adjusted between 0.12 and 1.20 mA to control the dose rate. The samples were placed on an AlN ceramic heater (WALN-3H, Sakaguchi) capable of heating from 40 to 500 °C. All measurements were conducted at room temperature.

3. Results and Discussion

Figure 1(a) shows the XRD patterns of Eu-doped $CaSiO_3$ samples with varying Eu concentrations (0.02, 0.05, 0.1, 0.2, and 0.5 mol%) and the reference pattern for $CaSiO_3$ (PDF 00-002-0506). A comparison of the measured and reference patterns revealed a good match, confirming that all the synthesized samples were obtained as single-phase $CaSiO_3$. No secondary phases or diffraction peaks originating from Eu were observed, even in the sample with the highest Eu concentration (0.5%). Given the similar ionic radii of Eu^{3+} and Ca^{2+}, it is considered that the Eu substitutes the Ca sites.

Figure 1(b) shows the PL spectra of the 0.1% Eu-doped $CaSiO_3$ sample before and after X-ray irradiation, together with the difference spectrum (inset). The latter concentration was selected as a representative since it exhibited the highest sensitivity. Although the extent of spectral change varies with Eu concentration, the overall trend induced by X-ray irradiation is independent of doping concentration. It is illustrated that the emission intensity of Eu^{3+} decreases with increasing X-ray dose whereas a broad emission band peaking at 640 nm appears upon X-ray irradiation and the intensity increases with dose. Comparable RPL properties, manifested as a broad emission in the same spectral range upon X-ray irradiation, have been reported in previous studies on Eu-doped Ca_2SiO_4.(17) Although the host material in this study is different, both show similar behavior in that a broad emission at around 600 nm appears after

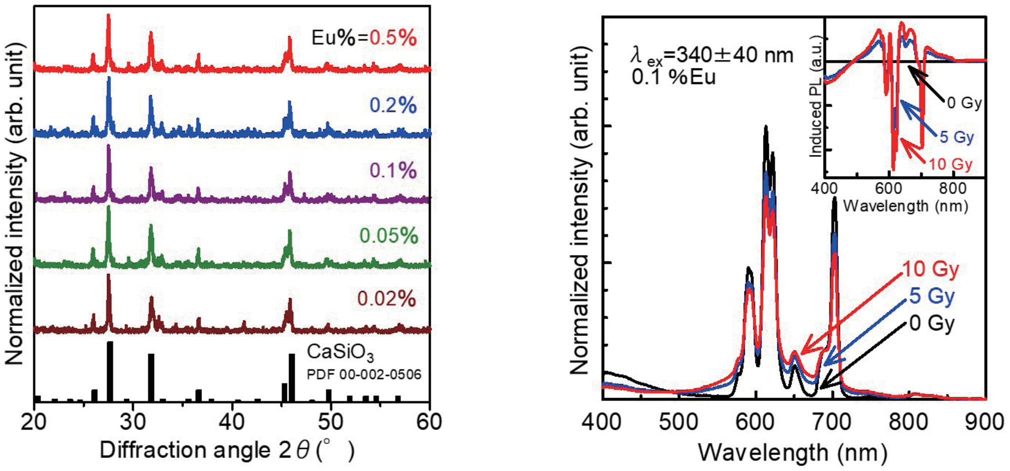

(a) (b)

Fig. 1. (Color online) (a) XRD patterns of Eu-doped $CaSiO_3$ samples as well as a reference pattern (PDF 00-002-0506). (b) PL spectra of 0.1% Eu-doped $CaSiO_3$ measured as a function of X-ray irradiation dose. The inset shows the difference spectra.

irradiation. Since prior research has attributed this emission to the 5d–4f transition of Eu^{2+}, our results suggest that the emission obtained in this study likely has the same origin. The underlying mechanism of RPL is thought to be caused by a capture of X-ray-generated electrons by Eu^{3+}, reducing the oxidation state to Eu^{2+}. This observation suggests the formation of a new luminescence center owing to ionizing radiation, and Eu-doped $CaSiO_3$ exhibits RPL properties.

With the RPL properties confirmed, the fundamental evaluations of the material were conducted. First, the dependence of RPL sensitivity on Eu doping concentration was investigated. By comparing the responses after 5 Gy of irradiation, we found that doping with 0.1% of Eu leads to the highest sensitivity (not shown). Next, to explore the dosimetric property, the dose response characteristics of the 0.1% Eu-doped sample were investigated. The result is shown in Fig. 2(a). Here, the RPL response is defined as an integrated PL signal in the 500–570 nm range induced by X-ray irradiation. The latter range was selected to avoid an overlap with the emission signal of Eu^{3+}. The PL intensity of Eu^{2+} increases monotonically with dose at least up to 10 Gy, showing an excellent dose response. The lowest detection limit, determined by the intersection with the 3σ line, is approximately 0.18 Gy. This suggests that this material can be used for dose measurements at least in the range from 0.18 to 10 Gy.

Subsequently, the stability of the generated Eu^{2+} centers was evaluated. Figure 2(b) shows the RPL response values measured every minute for 20 min after a 10 Gy irradiation. The response value stabilized after about 10 min, with a decay of only about 7% after 20 min. This indicates that the generated Eu^{2+} centers are considerably stable. With the same measurement system, the detection limit of a commercial Ag-doped phosphate glass is about 3 mGy,(18) whereas that of the present Eu-doped $CaSiO_3$ is about 180 mGy, indicating roughly 60 times lower sensitivity. However, the present material exhibits no significant build-up or fading at room temperature, which is significant for Ag-doped phosphate glass, suggesting an advantage for applications in real-time dosimetry.

The RPL response can be affected by heating at high temperatures. Figure 3(a) shows the PL spectra of 0.1% Eu-doped $CaSiO_3$ as a function of heat-treatment temperature. The sample was first irradiated with 10 Gy of X-rays and then thermally treated for 100 s. The PL spectrum was

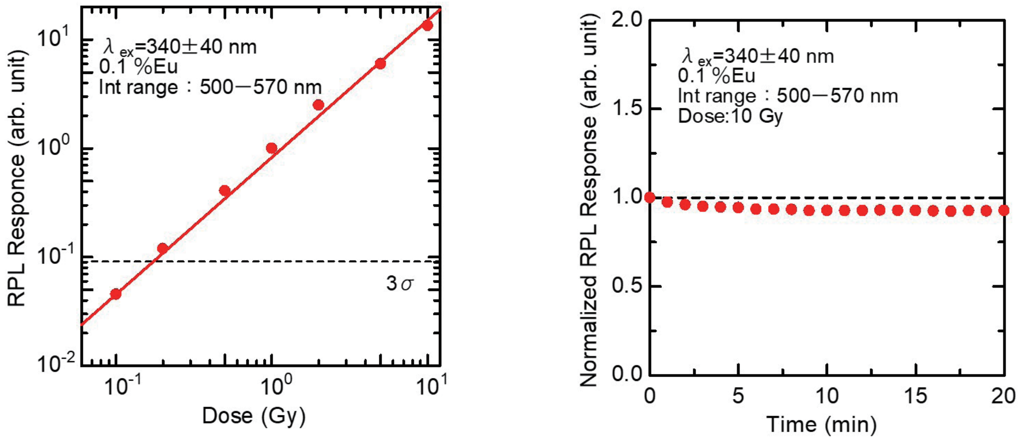

(a) (b)

Fig. 2. (Color online) (a) Dose response function of 0.1% Eu-doped $CaSiO_3$. (b) Relative RPL response as a function of elapsed time after X-ray irradiation (10 Gy).

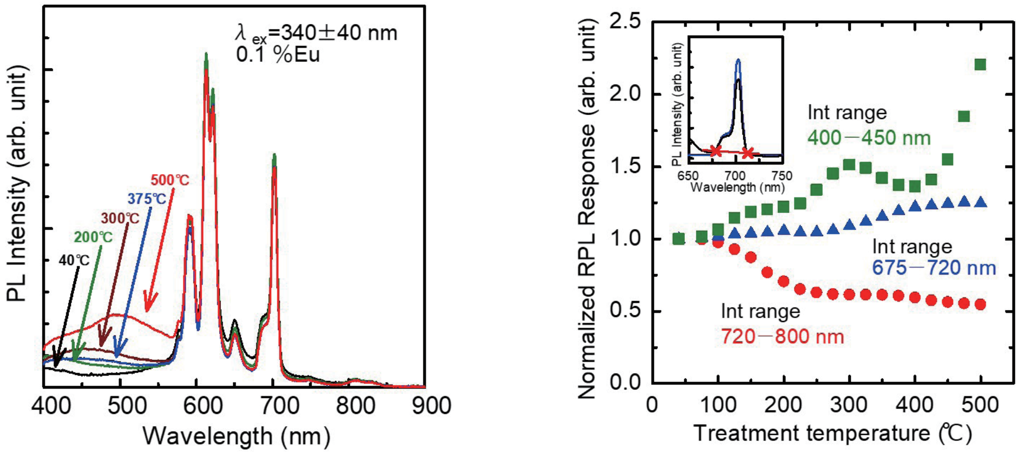

(a) (b)

Fig. 3. (Color online) Effects of heat-treatment temperature. (a) PL spectra of 0.1% Eu-doped CaSiO3 after X-ray irradiation as a function of treatment temperature. (b) Extracted PL intensities of defect center (400–450 nm), Eu^{2+} (720–800 nm), and Eu^{3+} (675–720 nm). All the PL measurements were performed at room temperature, the heat treatment time was 100 s, and the X-ray irradiation dose was 10 Gy.

measured at room temperature after every treatment. The results confirm changes in the PL spectra affected by thermal treatment. Note that a broad emission band appears in the shorter wavelength region. To analyze the effect of treatment in detail, the signal was separated into three spectral regions: 400–450, 720–800, and 675–720 nm to represent the signals of the latter new broad band, Eu^{2+}, and Eu^{3+}, respectively. The signal of Eu^{3+} was derived by linear baseline correction techniques, as illustrated in the inset of Fig. 3(b). Figure 3(b) shows these three signals as a function of treatment temperature. The new broad emission band shows a remarkable increase at around 300 °C and temperatures higher than 400 °C. A similar dependence on high-temperature heat treatment was confirmed even in undoped samples (not shown). This suggests that the origin of the new broad emission band is primarily attributed to defects generated in the host material. The PL signal of Eu^{2+} effectively decreases with increasing treatment temperature, whereas the Eu^{3+} signal increases. The observation suggests that the valence state of Eu^{2+} is reversed to Eu^{3+} during the heat treatment.

4. Conclusions

In this study, Eu-doped $CaSiO_3$ samples with various Eu concentrations (0.02–0.5 mol%) were synthesized by a conventional solid-state reaction method. XRD analysis confirmed that all the samples possessed a single-phase $CaSiO_3$ structure. Upon X-ray irradiation, an increase in PL intensity was observed, indicating RPL behavior. This luminescence is attributed to the formation of Eu^{2+} ions, which are generated as electrons produced by ionizing radiation captured by Eu^{3+} ions. The PL intensity originating from Eu^{2+} increases proportionally with the radiation dose and exhibits high stability even after irradiation. Furthermore, heat treatment induces significant changes in the PL spectra, accompanied by the appearance of a new broad emission band in the shorter wavelength region. Detailed spectral analysis revealed a decrease in the

Eu^{2+}-related emission and an increase in the Eu^{3+} emission, suggesting that Eu^{2+} ions are oxidized to Eu^{3+} during the heat treatment. The broad emission band becomes prominent at around 300 ℃ and above 400 ℃ and is also observed in undoped samples, implying that it originates from defects generated within the host material.

Acknowledgments

This work was supported by a Grant-in-Aid for Scientific Research (B) (22H02009) from the Ministry of Education, Culture, Sports, Science and Technology of Japan (MEXT), Shibuya Science Culture and Sports Foundation, as well as the Research Center for Biomedical Engineering. Also, a part of this work was performed as joint research with the Nuclear Power Safety Technology Research Center of Chubu Electric Power Co., Inc.

References

1 G. Okada: J. Ceram. Soc. Jpn. **129** (2021) 419. https://doi.org/10.2109/jcersj2.21056

2 T. Yanagida, G. Okada, T. Kato, D. Nakauchi, and N. Kawaguchi: Radiat. Meas. **158** (2022) 106847. https://doi.org/10.1016/j.radmeas.2022.106847

3 K. Shinsho: Phosphors for Radiation Detectors, T. Yanagida and M. Koshimizu, Eds. (Wiley, Hoboken, 2022) Chap. 7. https://doi.org/10.1002/9781119583363.ch7.

4 G. Okada, T. Yanagida, H. Nanto, and S. Kasap: Phosphors for Radiation Detectors, T. Yanagida and M. Koshimizu, Eds. (Wiley, Hoboken, 2022) Chap. 9. https://doi.org/10.1002/9781119583363.ch9.

5 R. Yokota and H. Imagawa: J. Phys. Soc. Jpn. **23** (1967) 1038. https://doi.org/10.1143/JPSJ.23.1038

6 T. Yamamoto, Y. Yanagida-Miyamoto, T. Iida, and H. Nanto: Radiat. Meas. **136** (2020) 106363. https://doi.org/10.1016/j.radmeas.2020.106363

7 Y. Miyamoto, Y. Takei, H. Nanto, T. Kurobori, A. Konnai, T. Yanagida, A. Yoshikawa, Y. Shimotsuma, M. Sakakura, and K. Miura: Radiat. Meas. **46** (2011) 1480. https://doi.org/10.1016/j.radmeas.2011.05.048

8 A. Mrozik, P. Bilski, B. Marczewska, B. Obryk, K. Hodyr, and W. Gieszczyk: Radiat. Meas. **71** (2014) 31. https://doi.org/10.1016/j.radmeas.2014.05.013

9 M. S. Akselrod, A. E. Akselrod, S. S. Orlov, S. Sanyal, and T. H. Underwood: J. Fluoresc. **13** (2003) 503. https://doi.org/10.1023/B:JOFL.0000008061.71099.55

10 V. Martin, G. Okada, D. Tonchev, G. Belev, T. Wysokinski, D. Chapman, and S. Kasap: J. Non-Cryst. Solids **377** (2013) 137. https://doi.org/10.1016/j.jnoncrysol.2012.12.015

11 Y. Kohara, G. Okada, I. Tsuyumoto, and H. Nanto: J Mater Sci: Mater Electron **34** (2023) 472. https://doi.org/10.1007/s10854-022-09759-5

12 G. Okada, K. Shinozaki, D. Shiratori, N. Kawaguchi, and T. Yanagida: Ceram. Int. **45** (2019) 9376. https://doi.org/10.1016/j.ceramint.2018.08.027

13 Y. Fujimoto, G. Okada, D. Sekine, T. Yanagida, M. Koshimizu, H. Kawamoto, and K. Asai: Radiat. Meas. **133** (2020) 106274. https://doi.org/10.1016/j.radmeas.2020.106274

14 K. Lin, W. Zhai, S. Ni, J. Chang, Y. Zeng, and W. Qian: Ceram. Int. **31** (2005) 323. https://doi.org/10.1016/j.ceramint.2004.05.023

15 M. K. Raju, P. Yadav, M. Gangadhar, S. Patel, R. K. Samudrala, A. Kumari, M. Bramanandam, and P. A. Azeem: Results Chem. **11** (2024) 101838. https://doi.org/10.1016/j.rechem.2024.101838

16 G. Okada, K. Hirasawa, T. Yanagida, and H. Nanto: Sens. Mater. **33** (2021) 2117. https://doi.org/10.18494/sam.2021.3327

17 S. Asada, G. Okada, T. Kato, F. Nakamura, N. Kawano, N. Kawaguchi, and T. Yanagida: Chem. Lett. **47** (2018) 59. https://doi.org/10.1246/cl.170940

18 G. Okada, W. Shinozaki, S. Ueno, Y. Koguchi, K. Hirasawa, F. d'Errico, T. Yanagida, S. Kasap, and H. Nanto: Jpn. J. Appl. Phys. **61** (2022) SB1035. https://doi.org/10.35848/1347-4065/ac1ab2